17th International Conference on the Application of Computer
Science and Mathematics in Architecture and Civil Engineering
K. Gürlebeck and C. Könke (eds.)
Weimar, Germany, 12–14 July 2006

INVERSE MODELLING OF SOIL HYDRAULIC CHARACTERISTIC FUNCTIONS

E. Stoimenova[*], **Y. Lins**[**], **M. Datcheva**[**] [+] **and T. Schanz**[**]

[*]*Institute of Mathematics and Informatics, BAS*
G. Bontchev 8, 1113 Sofia, Bulgaria
e-mail: jeni@math.bas.bg
[**]*Laboratory of Soil Mechanics, Bauhaus–Universität Weimar*
Coudraystr. 11c, D-99423, Germany
[+] on leave from *Institute of Mechanics, BAS*
G. Bontchev 4, 1113 Sofia, Bulgaria

Keywords: unsaturated soil, SWCC, nonlinear regression, inverse analysis

Abstract. *In this paper we evaluate 2D models for soil-water characteristic curve (SWCC), that incorporate the hysteretic nature of the relationship between volumetric water content θ and suction ψ. The models are based on nonlinear least squares estimation of the experimental data for sand. To estimate the dependent variable θ the proposed models include two independent variables, suction and sensors reading position (depth d in the column test). The variable d represents not only the position where suction and water content are measured but also the initial suction distribution before each of the hydraulic loading test phases. Due to this the proposed 2D regression models acquire the advantage that they: (a) can be applied for prediction of θ for any position along the column and (b) give the functional form for the scanning curves.*

1 INTRODUCTION

Most important relation to describe unsaturated soil behavior is the soil-water characteristic curve (SWCC), also known as retention curve in the field of soil science or capillary pressure–saturation relationship. In the present article we give experimental and statistical assessment to the SWCC of sand. For sand SWCC describes the relationship between the gravimetric water content, degree of saturation or volumetric water content and the matric suction or capillary pressure. Osmotic component of soil suction plays negligible role for sand therefor it is not considered hereafter in the presented study. The importance of SWCC is not only in giving insight of soil-water interaction but it is used to estimate the hydraulic conductivity and the shear strength, which are subsequently used in the modelling of water flow and stability analysis in geotechnical problems.

The relationship between water content and suction is hysteretic and this fact is presented by the existing of primary curves (the initial drying, the boundary wetting and the boundary drying curves) and an infinite number of scanning curves inside the hysteresis loop. A recent review and classification of hysteretic SWCC models is given in [1].

Direct determination of the SWCC from experiments on sand is difficult to handle due to the narrow soil suction range within which the water saturation and desaturation take place. Thus the suction range of readings relevant to the SWCC relationship is relatively small in comparison to the suction measurements error. That is why the assessment of the error and model verification and validation are of a critical importance in building up the SWCC relationship for sand.

In the present article we first give the experimental evidence related to the SWCC for sand. Afterwards using the available data a methodology is proposed for statistical assessment of the relationship between volumetric water content and suction. The main value of the method is the suggestion to add reading position d to the SWCC model as independent variable. Reading position represents the particular pair sensors that measures ψ and θ as well as the initial condition for the scanning curves. This way the obtained 2D SWCC models allow to better assess the measurement error and also provide functional form for the scanning curves.

2 EXPERIMENTAL PROCEDURE

In the Laboratory of Soil Mechanics at the Bauhaus-Universität Weimar, Germany a constant flow test has been done for determining soil water characteristic curve (SWCC) and hydraulic conductivity function (HCF) for Hostun sand [2]. The device comprises of a hollow plexiglass tube with an internal diameter of $30.5\,cm$ and a height of $67\,cm$. A flow pump is connected to the water reservoir below the column to impose a constant flow rate and to withdraw or to inject pore water depending on whether drying or wetting path is chosen. The flux rate range for the pump is from 10 to $150\,ml/min$. Burettes attached to the column monitor the rise and fall in water level during the test. The water lift in the burettes also is intended to indicate the complete saturation and desaturation of the sand column. During the tests vertical settlements were measured by using an attached dial gage in order to quantify volume changes in the sand specimen while drying and wetting take place. For measuring the pore-water pressure five tensiometers are placed in a row along the column. To measure the volumetric water content at the same level as for the tensiometers the column is additionally instrumented with TDR (Time Domain Reflectometry) sensors. This way measurements of pore pressure and water content

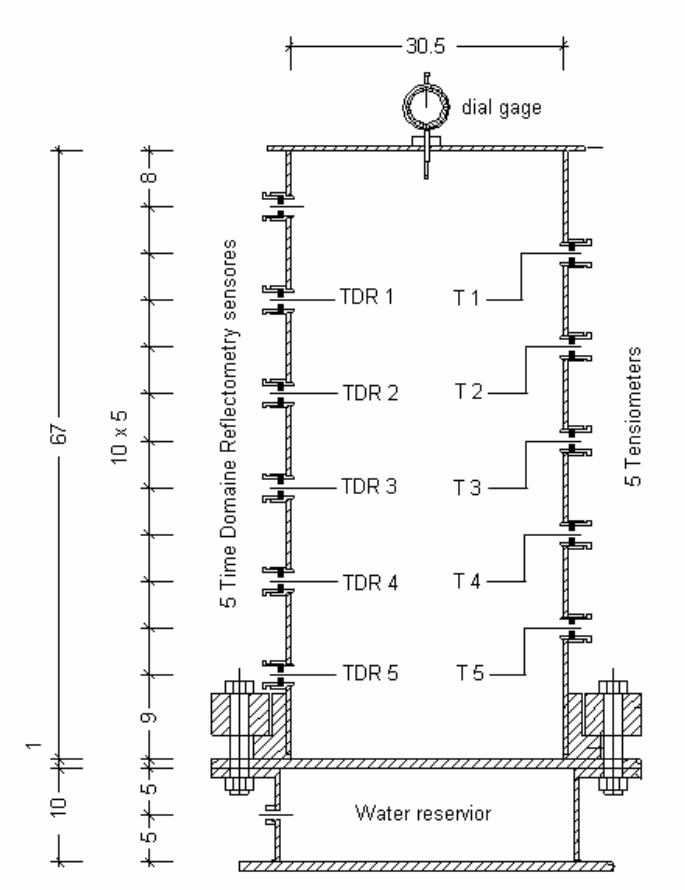

Figure 1: Cross section of the instrumented sand column

are taken at each $10\,cm$ along the sand column. A cross section through the column is depicted in Figure 1. Both tensiometer and TDR measurements during the continuous constant rate wetting or drying linked directly give the soil-water characteristic curve at five positions along the specimen (position 1 is at the top and position 5 is at the bottom). The tensiometers and TDRs are connected to a data logging system and to a computer for recording and analyzing the measurements.

Loose Hostun Sand specimen with void ratio 0.89 was prepared by pluviating sand into the column filled with deaired water, thus ensuring initial degree of saturation to be almost 1. Starting with an initially fully water saturated specimen, the sand was dried and wetted again by withdrawing and adding water from the specimen bottom with a flow rate of approximately $30\,ml/min$.

3 DATA INTERPRETATION

TDR readings as well as tensiometer measurements during the drying phase are given in Figure 2. The initial condition for the drying path is a fully water saturated specimen with water table located at the top of the specimen. Tensiometer T1 is located at the top and tensiometer T5 at the bottom of the column. At the beginning of the test tensiometer T5 measures higher positive pore-water pressure than tensiometer T1 and the reading is in accordance with the gravimetric water pressure distribution. The sand specimen is saturated and the measurements

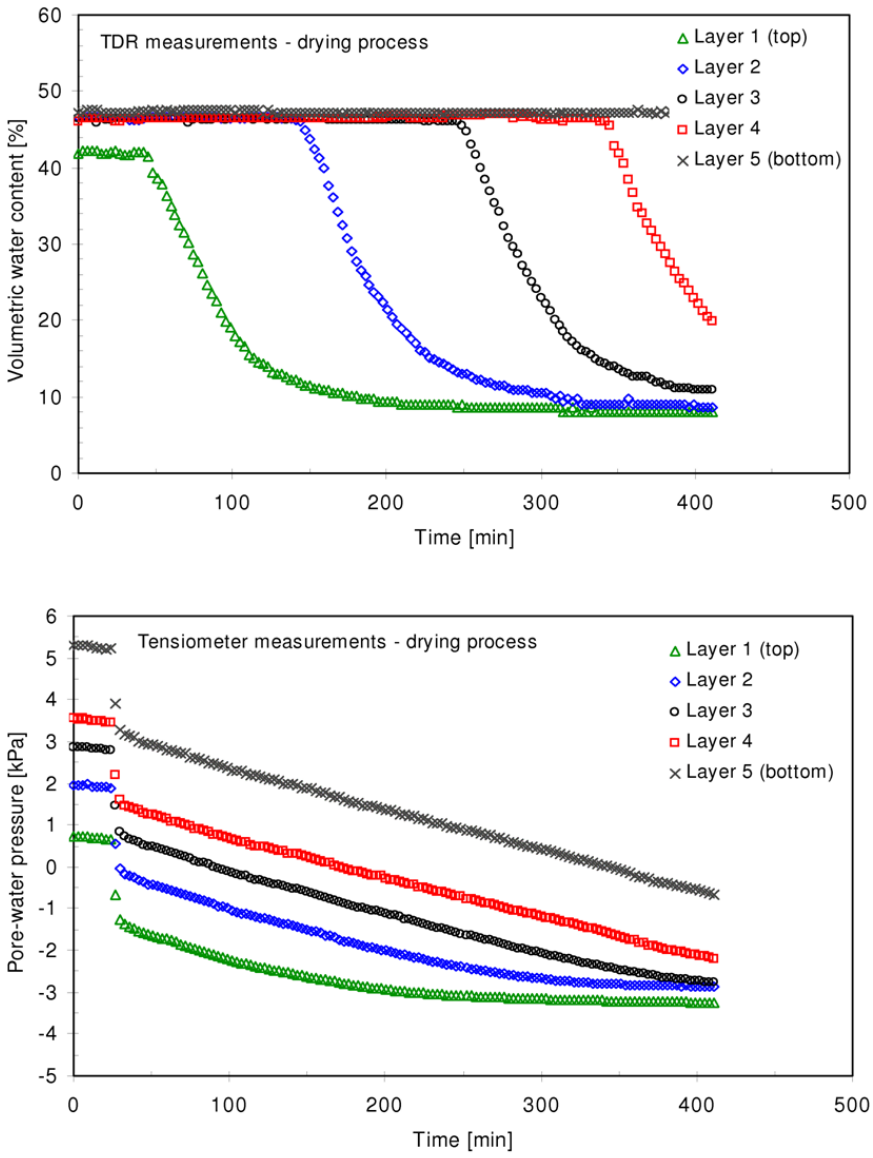

Figure 2: TDR measurements (top) and tensiometer measurements (bottom) from drying process

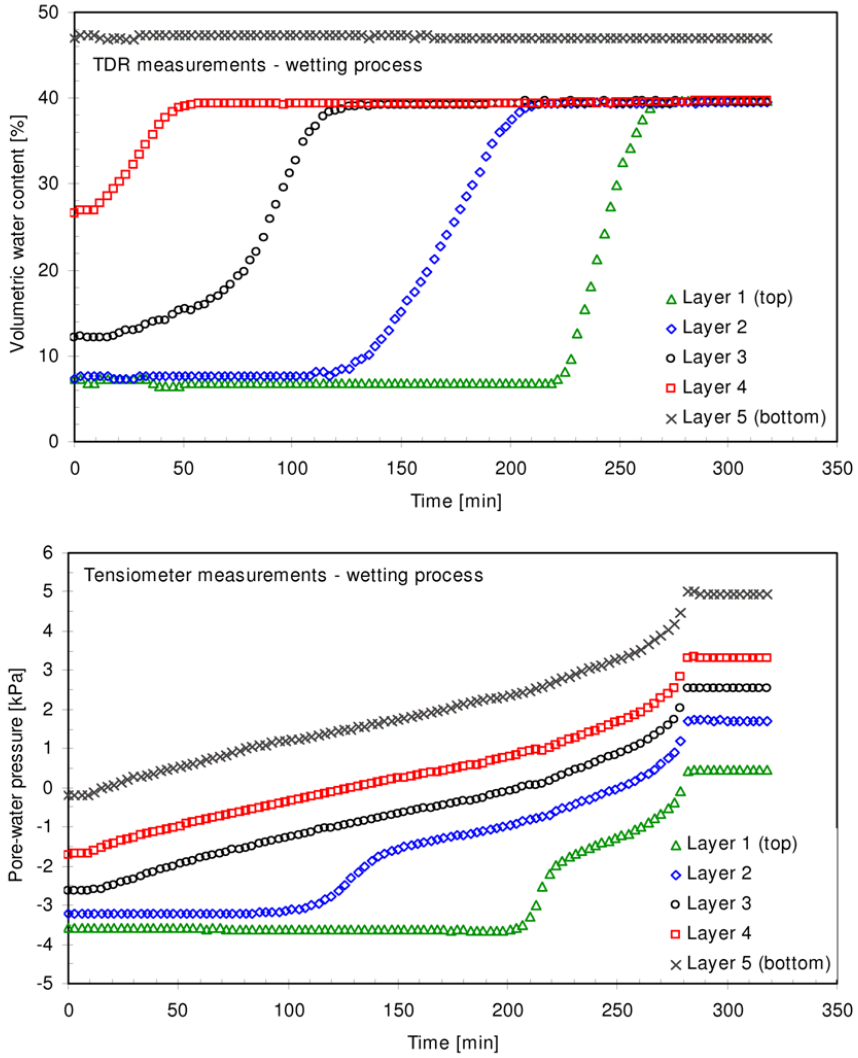

Figure 3: TDR measurements (top) and tensiometer measurements (bottom) from wetting process

of all TDR sensors correspond to degree of saturation equal to 1. During the drying process the positive pore-water pressures decrease starting from the upper part of the specimen. When at a given measuremet point the air intrudes the sand pore system the corresponding TDR sensor measures drop in the volumetric water content. The measurement of the tensiometers become negative when they are above the water level and in this case the measured pore water pressure is the matric suction. At the end of the drying process the matric suction is higher at the top of the specimen than at the bottom. During drying the volumetric water content is decreasing, first at top of the specimen and afterwards at the bottom of the specimen. For the first drying path the water has been pumped out until water table measured by burettes became below the specimen bottom. The specimen has been left for 65 hours to equilibrate before the first wetting test started. Even the sand column was above the water table the lower part of it has not been in unsaturated condition. The TDR5 reading indicates full saturation at this measurement point. The matric suction for each tensiometer was different and this is presented in Figure 3. The measured volumetric water content increases with depth. During the wetting path the matric suction is decreasing. Positive pore-water pressures are expected to be in accordance to the hydrostatic water pressure distribution. During the wetting process the volumetric water content

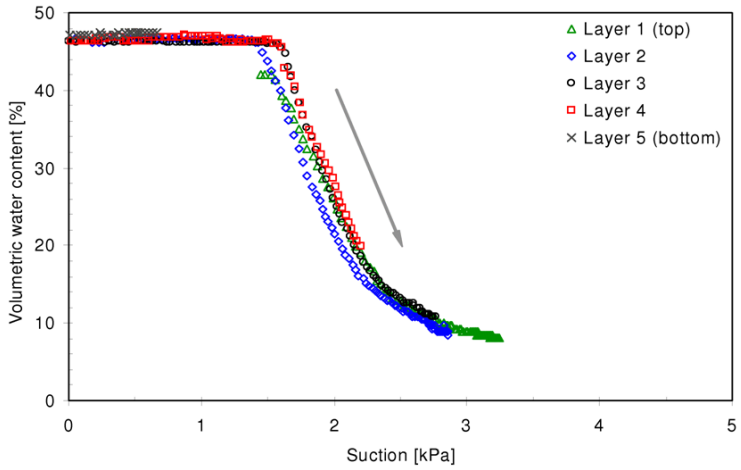

Figure 4: Experimental results from the first drying phase

increases starting from the bottom of the specimen. The wetting test is stopped when the water table reaches the top of the specimen. Even when the water table is at the top of the specimen, measurements of TDR1 to TDR4 refer to a degree of saturation less than 1. This reflects the fact that there are occluded air bubbles which are not possible to remove by the method to supply the specimen with water used in the test. Only TDR5 located at the bottom of the specimen measures a volumetric water content corresponding to full water saturated condition. The lowest portion of the specimen has remained saturated during the entire test duration and therefore no possibility was there for occluded air bubbles to occur. The sensors at the bottom of the column are situated in the saturated zone throughout the complete testing procedure. All the other sensors give readings for saturated as well as unsaturated conditions.

Readings of the tensiometers and the corresponding TDR probes give the data for the SWCC. SWCC data are depicted in Figure 4 for the first drying process and in Figures 5 and 6 for the first and second wetting paths. The fact that for the first drying path the initial condition at each measurement position is the same degree of saturation equal to 1 and suction equals to 0, results in almost coinciding curves. For wetting processes the initial condition for the saturation at each measurement point is different. The matric suction at the top of the specimen is higher than at the bottom of the specimen, which gives different wetting curves for different readings positions. These wetting curves are known as scanning curves.

During all the phases of the test the volume changes were measured and the data show negligible changes in the height of the sand column. That is why the void ratio has been considered to be almost constant when modelling SWCC.

The curves, for both first drying and second wetting tests, are shown in Figure 7. As can be seen in Fig. 7 the SWCC obeys hysteresic property during hydraulic loading-unloading cycle. Thus the water content for a given matric suction value corresponds during drying process to a higher matric suction then during wetting process. Hysteresis depends not only on loading history of the soil but also on the drying and wetting rate. Several reasons, as rain drop effect [3], ink-bottle effect [4] or snap-off effect are given in literature for the phenomenon of hysteresis. Here we do not go in detail discussion about the reasons for hysteretic form of the relationship between suction and volumetric water content as we are interested in functional representation of SWCC rather then in the hysteresis phenomenon itself.

For application of SWCC in solving geotechnical problems it is essential to include scanning

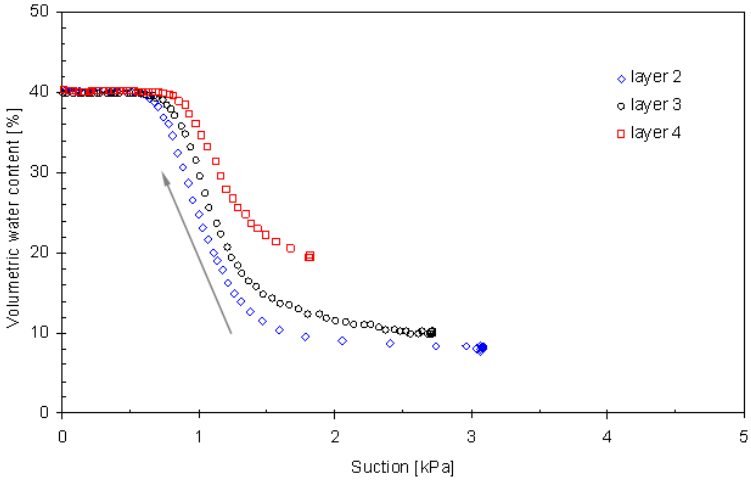

Figure 5: Experimental results from the first wetting phase

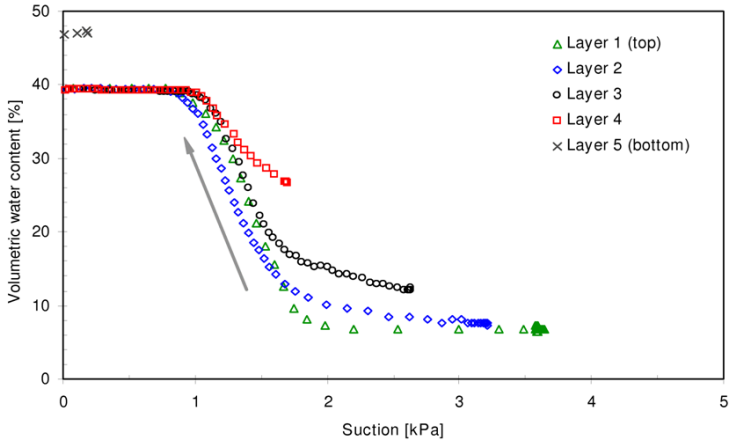

Figure 6: Experimental results from the second wetting phase

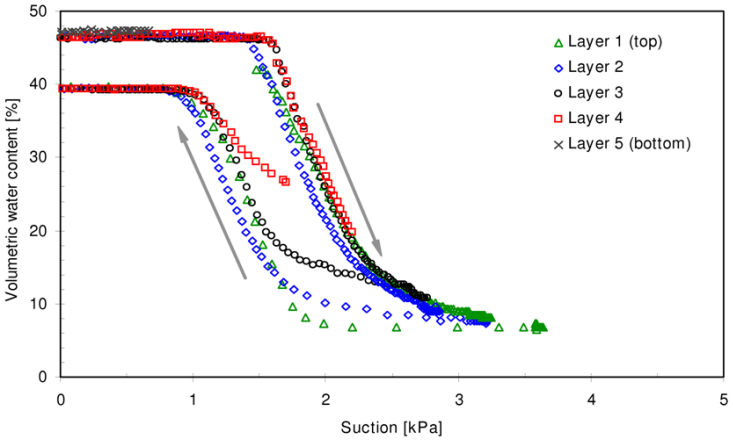

Figure 7: Experimental results from the first drying-wetting cycle

curves and hysteretic form of the relationship between volumetric water content and suction. This way the error induced by using a unique SWCC in cases when drying–wetting cycles are present can be avoided.

4 STATISTICAL ASSESMENT OF SOIL-WATER CHARACTERISTIC CURVE

In this section, a method to obtain information about the heterogeneity of the subsurface (inverse modelling) has been applied. Inverse models use measurements of variables that are related to the properties that are to be estimated.

Use of inverse models, such as nonlinear least-squares regression and associated statistics, facilitates assessment of prediction reliability because the results yield not only parameter estimates, but also confidence intervals for the estimated coefficients and proportion of the explained variance of the model. We use the Levenberg-Marquardt (LM) algorithm which is an improvement of the classic Gauss-Newton method for solving nonlinear least-squares regression problems. The method is discussed in detail in [5]. The LM method seeks $\hat{\beta}$, the solution of β (locally) minimizing:

$$g(\beta) = \sum_{j=1}^{m} \sum_{i=1}^{n} (\theta_i - f(\beta, \psi_i, d_j))^2$$

where ψ_i and θ_i are sets of measured suction and volumetric water content at different depths d_j. Both ψ and the depth d, at which the sensors are instrumented, are thought to be important factors for describing the systematic variation in the θ data. The cross sections of the data are given in Figure 4 for first drying phase, in Figure 5 for first and Figure 6 for the second wetting paths. Each cross-sectional plot shows the relationship between θ and ψ for a particular d (layers 1 to 5). The relationship between θ and ψ for each d consists of two parts: constant part for $\psi < aev$ and a part of nonlinear decreasing function for $\psi > aev$. The threshold aev gives the suction of air entry or air expulsion depending whether drying or wetting path is modeled.

The fact that the profiles of θ versus ψ vary with depth d confirms that any functional description of the process will need to include this variable. Further insight into the appropriate function to use can be obtained by separately modelling each cross-section of the data and then relating the individual models to one another. We use the procedure given in [6] to establish the cross-section models fitting the accepted stretched exponential relationship between θ and ψ. This way the following model is obtained:

$$\theta = \begin{cases} \alpha & \psi < aev \\ \beta_0 + \beta_3 \exp(-\dfrac{\psi^{\beta_1}}{\beta_2}) & \psi > aev \end{cases}$$

to each cross-section of the volumetric water content. Examining plots of the estimated parameters versus d roughly indicates how the position of measurement should be incorporated into the model of the data. Regression curves to the cross-sections data for the 1st wetting phase at three different positions are given in Figure 8.

The individual exponential fits to each cross-section of the data reveal the influence of sensors position d. Three of the estimated parameters are not sufficiently different for different layers while the scaling parameter β_3 is. Further, we tried to replace β_3 with a term expression depending on d which incorporates the variation of this parameter for different layers. Simple

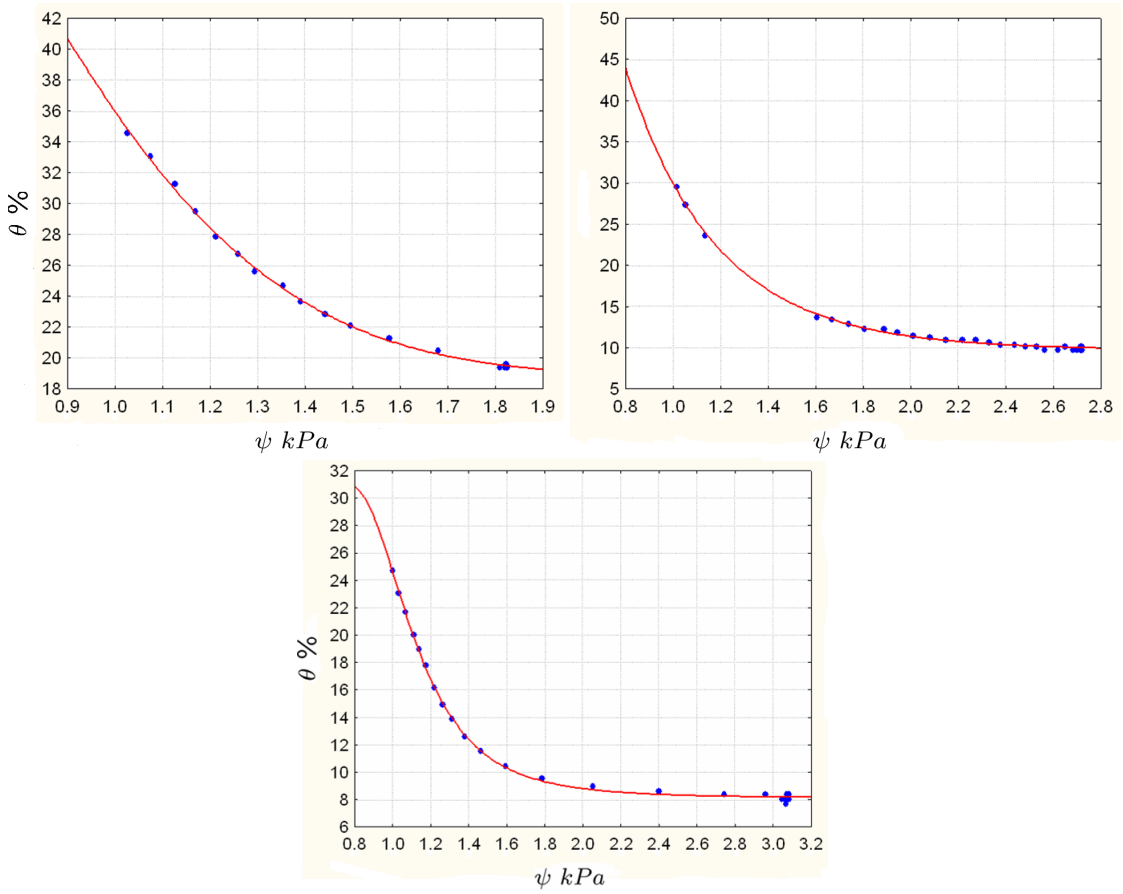

Figure 8: Cross-section fit for the 1st wetting phase: d=17.5; 26.8; 37 cm

linear term of d instead a constant β_3 showed the best fit over the trial models. The resulting model is:

$$\theta = \begin{cases} \alpha & \psi < aev \\ \beta_0 + (\beta_3^1 + \beta_3^2 d)\ \exp(-\dfrac{\psi^{\beta_1}}{\beta_2}) & \psi > aev \end{cases}$$

where d is the depth at which the measurement has been recorded. For applying the proposed methodology we exclude from the data those measurements taken at the bottom and the top of the specimen. This is because at the beginning of the first drying test the sample has been partly desaturated at the top and consequently resaturated. This way the reading data for the initial drying and first wetting paths for TDR1 - T1 sensors pair has been lost.

The fitting parameters are given in Table 1. Parameters are given without dimension as the suctaion is scaled with a reference suction of $1\,kPa$ and the depth with a reference length of $1\,cm$. Resulting 2D model for the first drying is depicted in Figure 9. Figure 11 shows the 2D models for the first and second wetting phases.

We use different statistical techniques to validate the model. Several plots of the residuals from a fitted model are used to see the adequacy of different aspects of the model. All of them do not show an essential departure from the model. Figures 10, 12, 13 depict the outcome from the residual analysis for the three test phases used in building the 2D models.

Numerical methods for model validation, such as proportion of explained variation, give enough support to use the model equation for predicting θ with sufficient small error. The

Table 1: Estimated model parameters for the 2D models

	aev	α	β_0	β_1	β_2	β_3^1	β_3^2
1st drying	1.5	46.26	46.49	-7.61	0.01	-28.18	-0.29
1st wetting	0.7	39.97	43.40	-3.24	1.14	-32.,67	-0.20
2nd wetting	0.9	39.38	43.50	-3.76	0.4	-31.97	-0.30

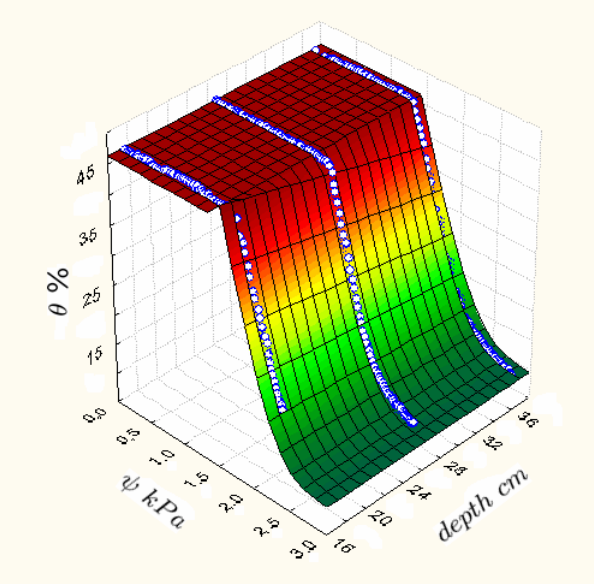

Figure 9: 3-D Plot of observed and predicted θ for the first drying path.

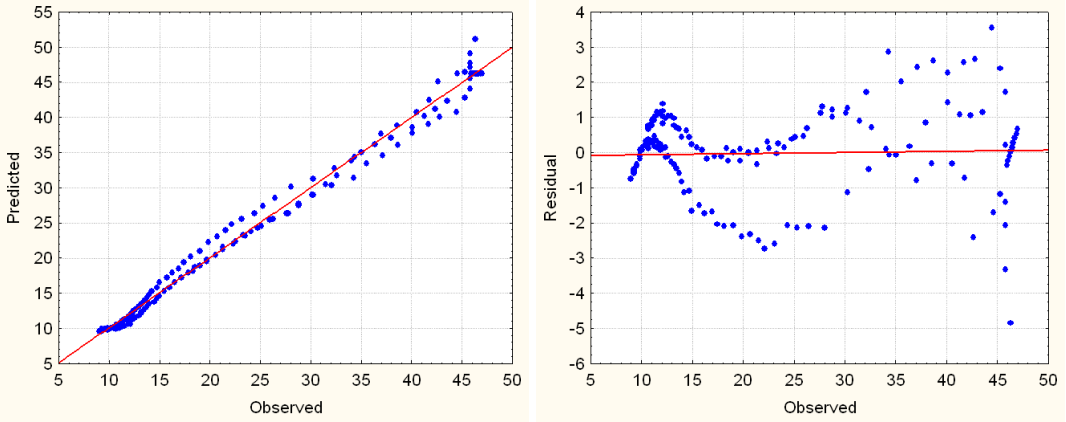

Figure 10: Residual analysis for the 1st drying path: predicted vs observed (left) and residual vs observed (right).

values of this proportion (or R^2 of nonlinear regression) are very similar for the three tests data: first drying – 0.977, first wetting – 0.976, second wetting – 0.980.

5 CONCLUSIONS

The goals of process modelling, answering a scientific or engineering question, depend on the correctness of the process model. The basic steps used for model building are the same

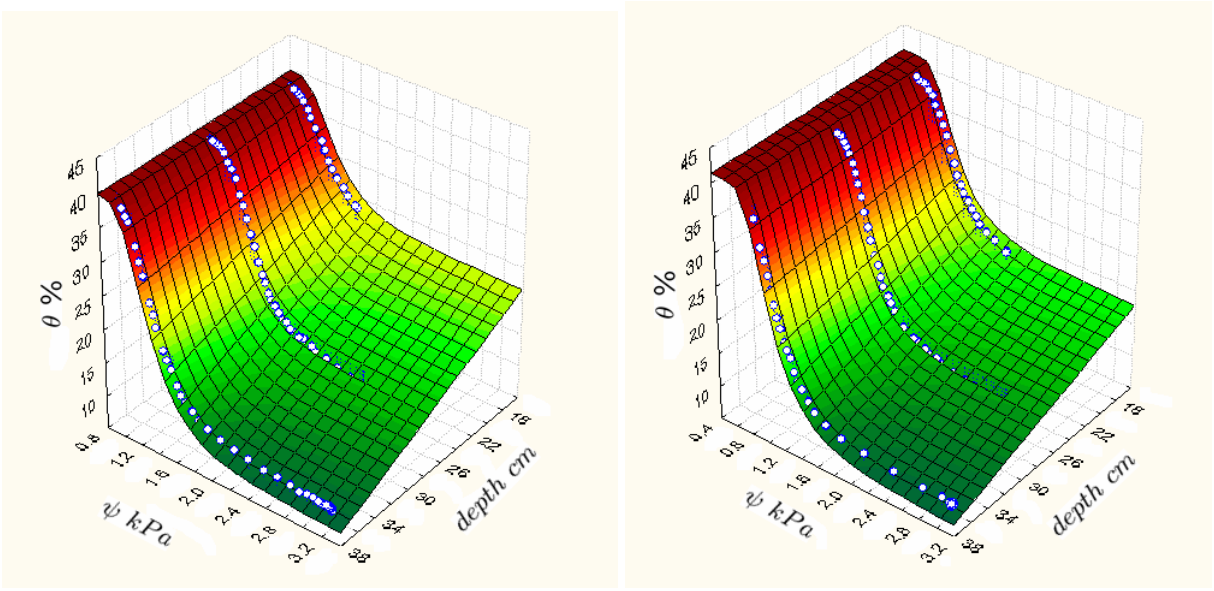

Figure 11: 3-D Plot of observed and predicted θ for the first(left) and second (right) wetting paths.

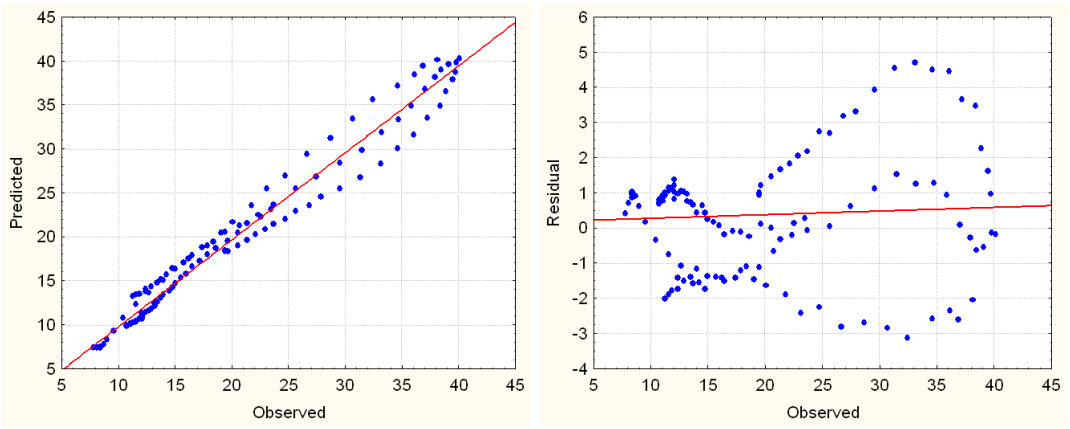

Figure 12: Residual analysis for the 1st wetting path: predicted vs observed (left) and residual vs observed (right).

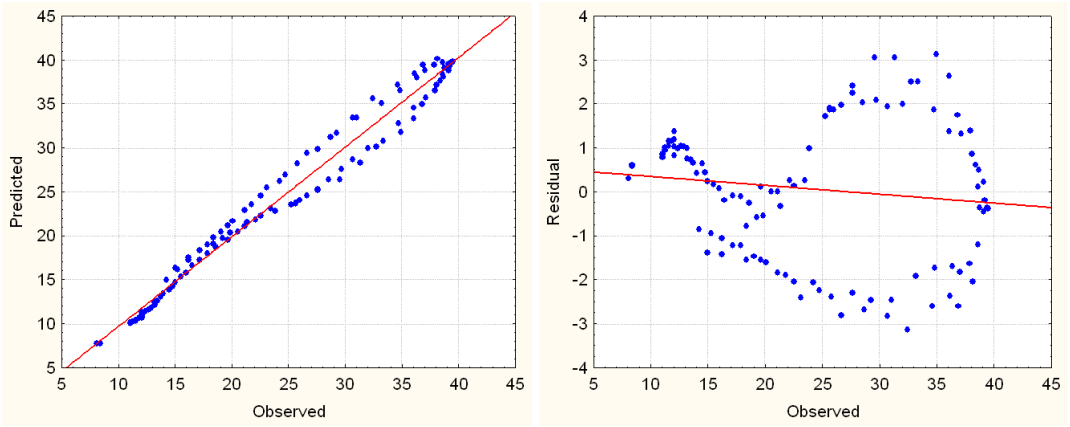

Figure 13: Residual analysis for the 2nd wetting path: predicted vs observed (left) and residual vs observed (right).

across all modelling methods. They usually include model selection, model fitting, and model validation. All the steps assume that the data has been already collected and the same data

can be used to fit all of the candidate models. In summary, the above presented results are an effort to access based on statistical analysis the hysteretic form of the SWCC and to model scanning curves applying 2D statistical model. The available data contain measurement of the volumetric water content θ and suction ψ at five different levels within the sand column. The measurement errors are different at different levels. In this case, ψ and measurement depth d are used to obtain better estimates of soil properties, such as SWCC. Incorporating this available information about relationship θ - ψ, we construct a model that can be applied for prediction of θ for any position along the column. The uncertainty related to different measurement errors of TDR's is combined and used for estimating a global prediction error. The estimated error of the model is valid in entire interval of ψ-values and for arbitrary depth level.

Model validation is possibly the most important step in model building sequence. In the model selection step, plots of the data, process knowledge and assumptions about the process are used to determine the form of the model to be fitted to the data. We illustrate the construction of non-linear regression model for soil data following the methodology given in [6]. It demonstrates fitting a nonlinear model and the use of transformations to deal with violation of the assumption of constant standard deviations for the residuals.

Acknowledgement

This work has been supported by the German Research Foundation (DFG) under the grant FOR444 and the Bulgarian National Science Fund (Grant MM1301). The third author acknowledges the Thuringia HWP fellowship for having the possibility to take part in this research.

REFERENCES

[1] H. Q. Pham, D. G. Fredlund and S. L. Barbour , A study of hysteresis models for soil–water characteristic curves. *Can. Geotech. J.*,**42**, 1548–1568, 2005.

[2] Y. Lins, T. Schanz, D. G. Fredlund , Determination of the unsaturated hydraulic conductivity function for Hostun Sand using direct and indirect methods. *Can. Geotech. J.*,submitted, 2006.

[3] J. Bear, *Dynamics of fluids in porous media*. American Elsevier Publishing Company Inc., 1972.

[4] E. E. Miller and R. D. Miller, Physical theory for capillary flow phenomena. *Transport in porous media*, **3**, 324–332, 1988.

[5] J.–J. More, The Levenberg-Marquardt algorithm: Implementation and theory. In *Numerical Analysis, Lecture Notes in Mathematics*, 630, Springer Verlag, 1977.

[6] E. Stoimenova, M. Datcheva and T. Schanz, Statistical approach in soil-water characteristic curve modelling. *Springer Proceedings in Physics*, **93**/II , 189–200, 2005.